Supplementary Materials – Additional diagrams for:

”The Mesoarchean Amikoq Layered Complex of SW Greenland: Part 2. Geochemical evidence for high-Mg noritic plutonism through crustal assimilation”

Fig. S1. Supplementary field photos. **a)** Dark, angular mafic amphibolite block (supracrustal origin?), hosted in noritic rocks at West Margin. **b)** Sub-vertical layering in peridotite at West Margin – whether igneous or metamorphic is unclear. **c)** Typical knobbly texture in peridotite at West Margin, similar to that observed at Seqi (Szilas et al., 2018).

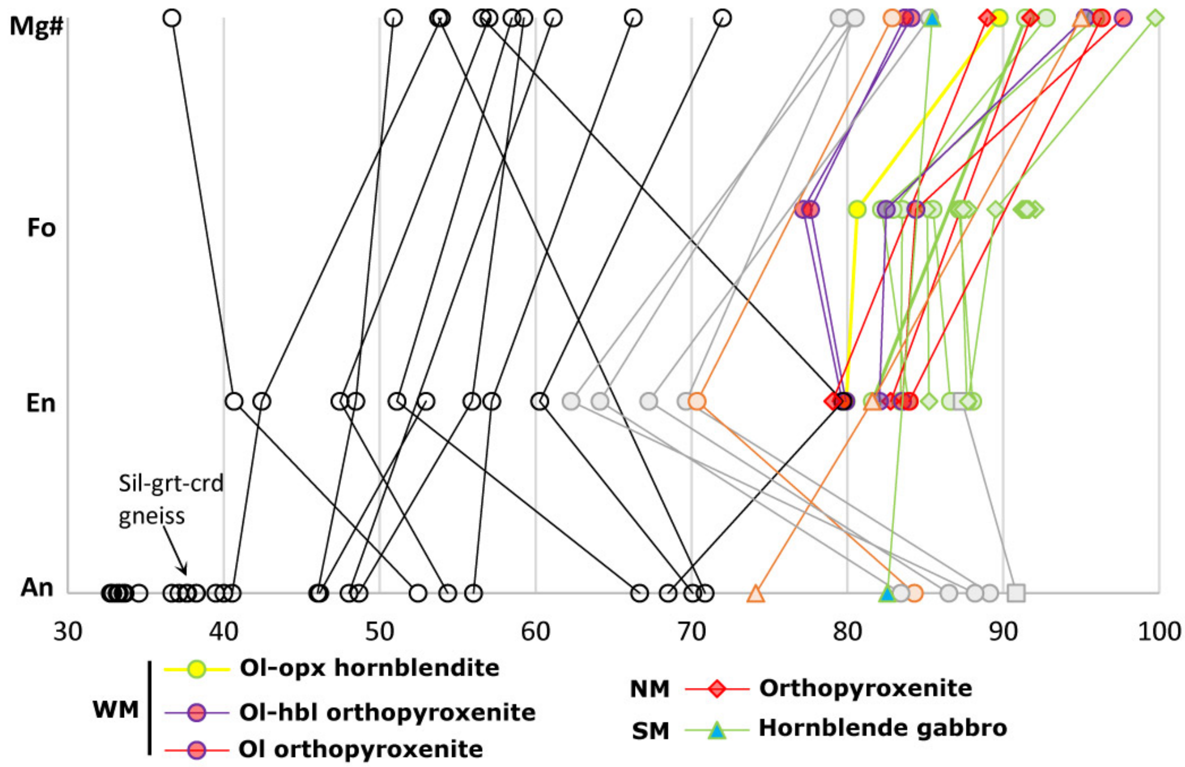

Fig. S2. Amikoq olivine-orthopyroxene-plagioclase-amphibole compositional data based on Aarestrup et al. (2020), Kristensen (2006) and Szilas et al. (2015). WM: western margin; NM: northern margin; SM: southern margin.

West Margin

(Not to scale)

	Olivine Forsterite (mol.%)	Opx Enstatite (mol.%)	Pl Anorthite (mol.%)	Cpx Mg#	Green Ca-amp Mg#	WR Mg#
Mafic supracrustal (roof)		48-60	47-70	59-67	57-72	21-33
Norite 2		70	89		80	42
Ultramafic	77-87	80-88		83	84-97	46-77
Orthopyroxenite lens 1		70	84		83	41
Norite 1		62-67	83-88		79-85	29-34
Marginal zone (Not to scale) – **K-hastingsite gneiss**			46	67	50	25
Aluminous gneiss			38			
Basal amphibolite						35
TTG gneiss						

South Margin

(Not to scale)

	Olivine Forsterite (mol.%)	Opx Enstatite (mol.%)	Pl Anorthite (mol.%)	Cpx Mg#	Green Ca-amp Mg#	WR Mg#
Mafic supracrustal (roof)		42	41	60	54	23-35
Ultramafic 2						64
Norite 1		82	77		95	53-61
Melagabbro			83		85	25-53
Ultramafic 1						61-64
Basement / TTG gneiss						

North Margin

(Not to scale)

	Olivine Forsterite (mol.%)	Opx Enstatite (mol.%)	Pl Anorthite (mol.%)	Cpx Mg#	Green Ca-amp Mg#	WR Mg#
Mafic supracrustal (roof)				58	54	12-25
Norite 2 – **Orthopyroxenite**		79-83			89-92	46-59
Norite 2		87	91			60
Norite 2 – **Ultramafic**	85	85				57-61
Mafic supracrustal 1						30
Norite 1						52-58
Norite 1 – **Ultramafic**	87					57-62
Aluminous gneiss						
Basal mafic supracrustal						
TTG gneiss						

Fig. S3. Schematic illustration of the stratigraphy at **a)** West Margin, **b)** South Margin and **c)** North Margin. The schematic logs are based on geological maps (Aarestrup et al., 2020), and currently available whole-rock and mineral data. Obvious metamorphic minerals are not included. Mafic host rock aka. supracrustal host rock. Data sources: Aarestrup et al. (2020), Kristensen (2006), Szilas et al. (2015).

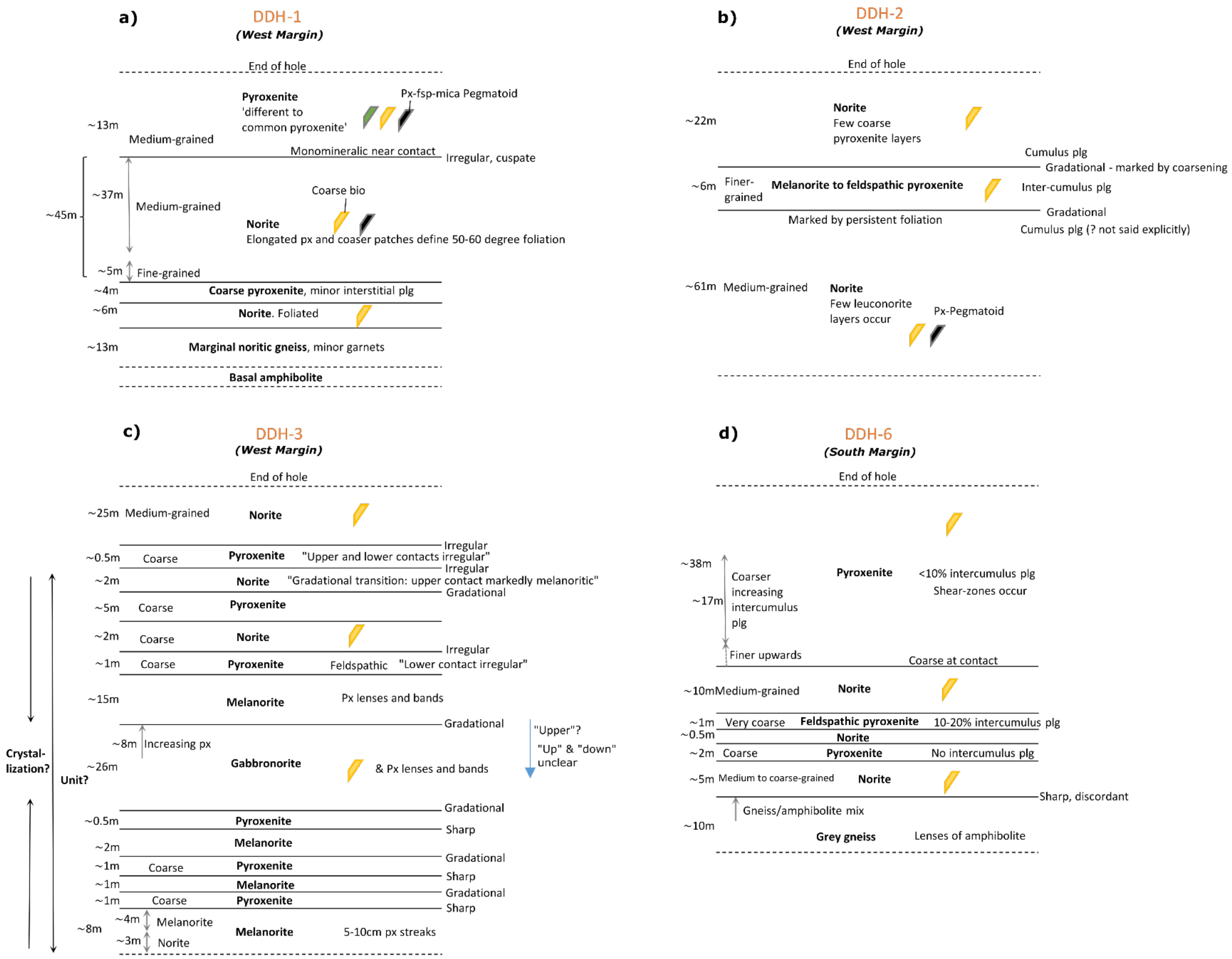

Fig. S4. Schematic illustration of drill cores (see **g-h** below for location of drill holes). 'Melanorite' and 'feldspathic pyroxenite' are encompassed under 'melanorite' in the main text. Whether the gabbronorite in **c)** is part of the igneous sequence or represent an intercalated amphibolite host rock remains to be validated. Even though some of the boreholes are closely spaced, it is not possible to correlate the logs.

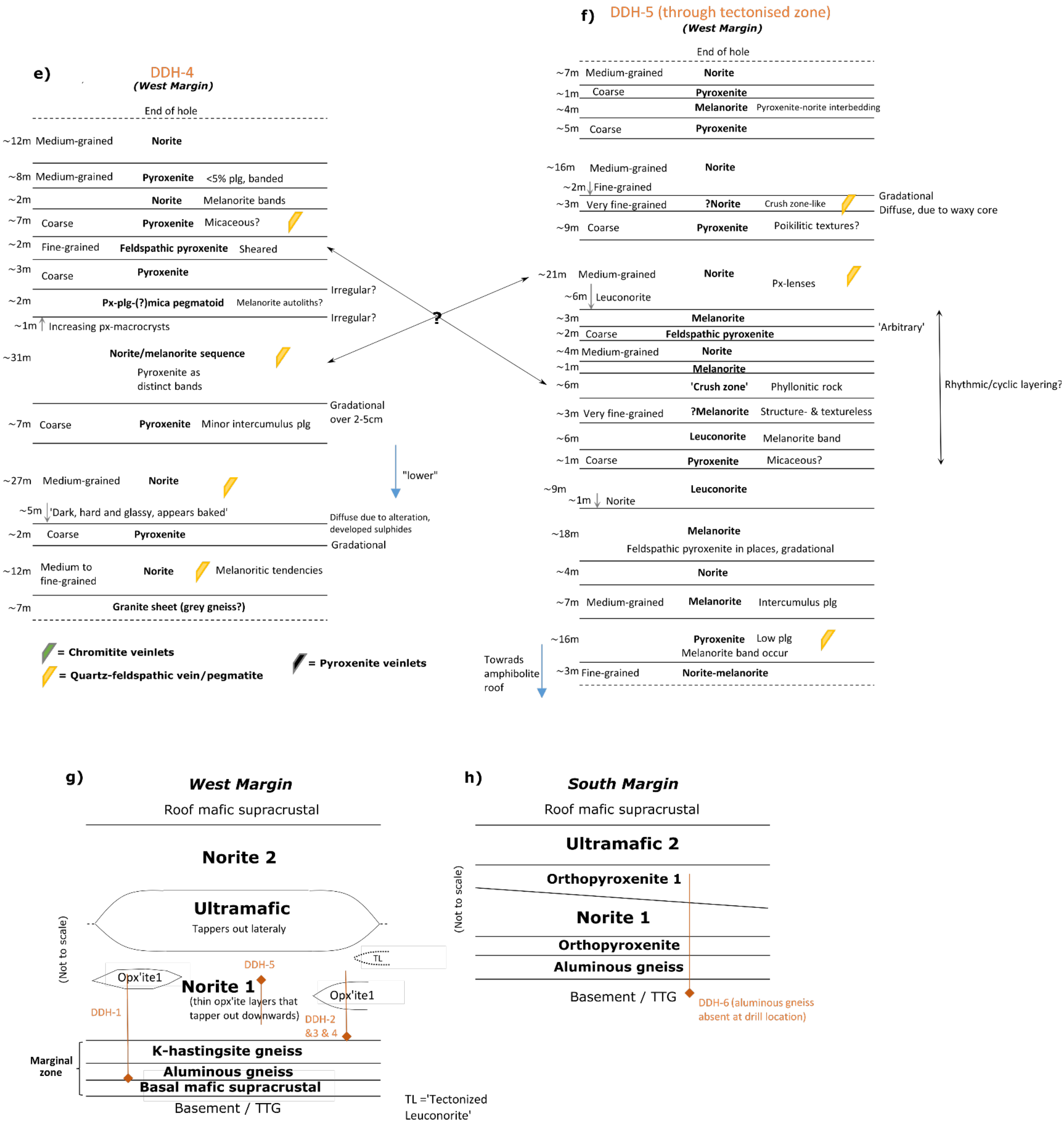

Fig. S4 (continued). Schematic illustration of drill cores from West Margin and South Margin.

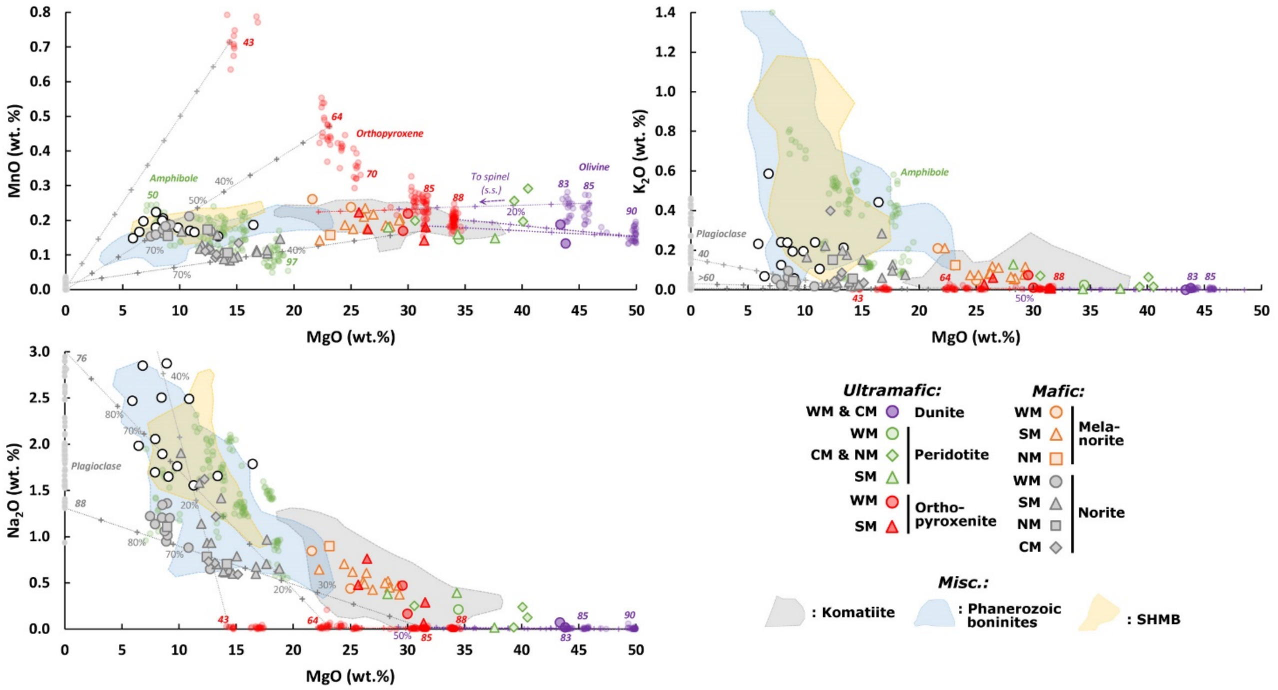

Fig. S5. Supplementary major element plots to Fig. 4 of the main text – for details, see main text and Fig. 4 caption.

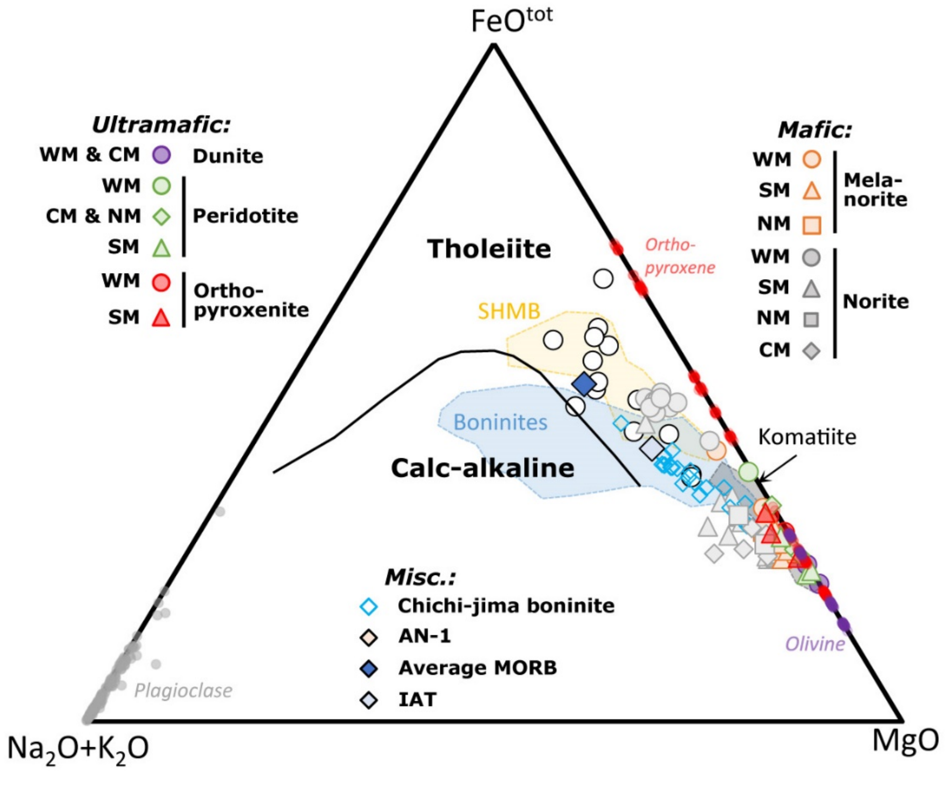

Fig. S6. Ternary K_2O+Na_2O, FeO_{tot}, MgO plot. The mafic host rock form a Fe-enrichment, tholeiitic trend. The locus of most ALC samples plot in the origin region for very primitive mantle derived melts.

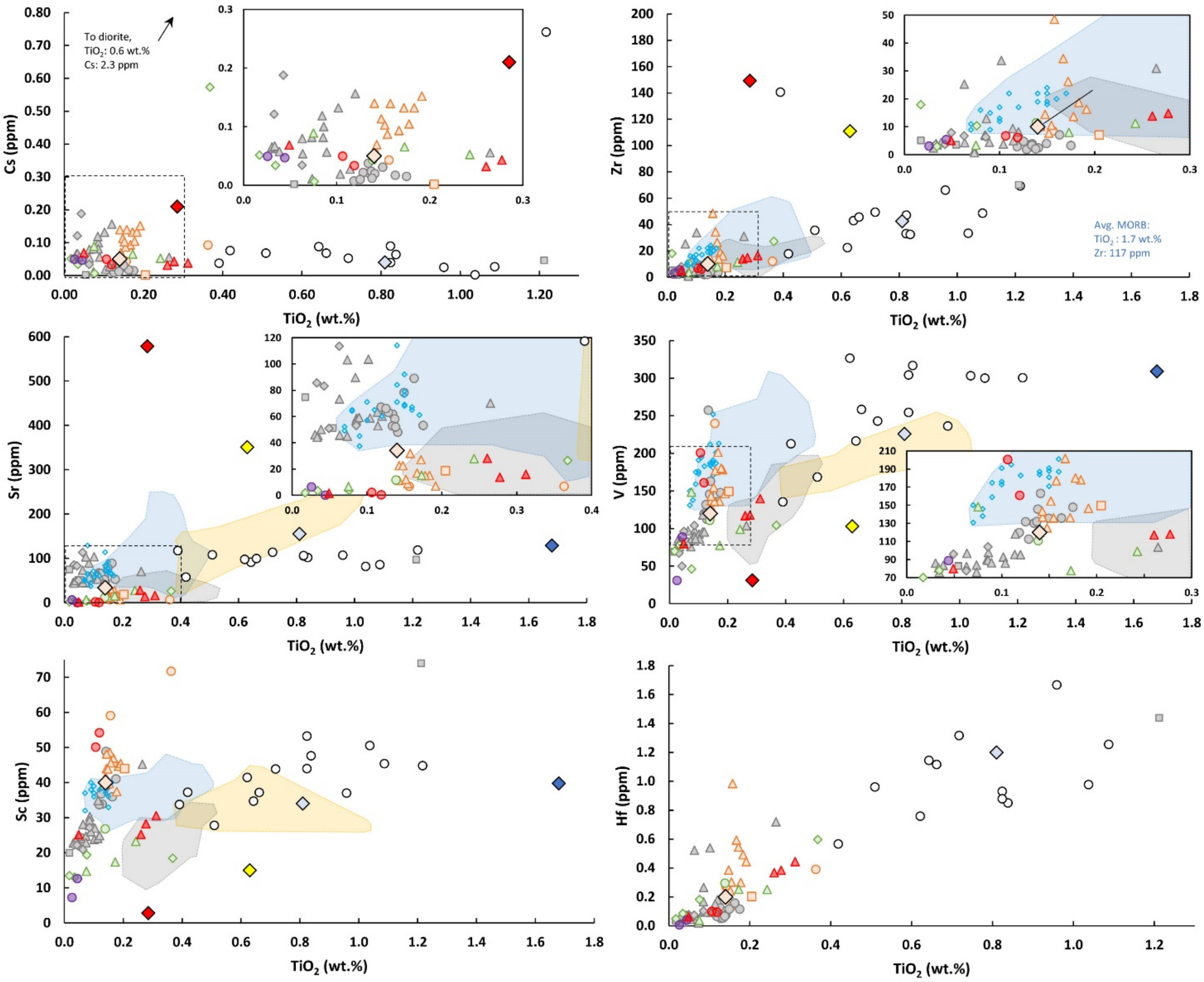

Fig. S7. Selected trace elements plotted against TiO_2 (wt.%). In most plots, the melanorites form a clear separate trend interpreted as a melt evolution trend. The Amikoq noritic parental melt (AN-1) is inferred to contain 0.14 wt.% TiO_2 and a complete melt composition may then be inferred. Some elements are better constrained than others, as some melanorite elements depict a blurry trend. Some major elements may partly be influenced by mineral accumulation. Symbols as in **Fig. 4** of the main text.

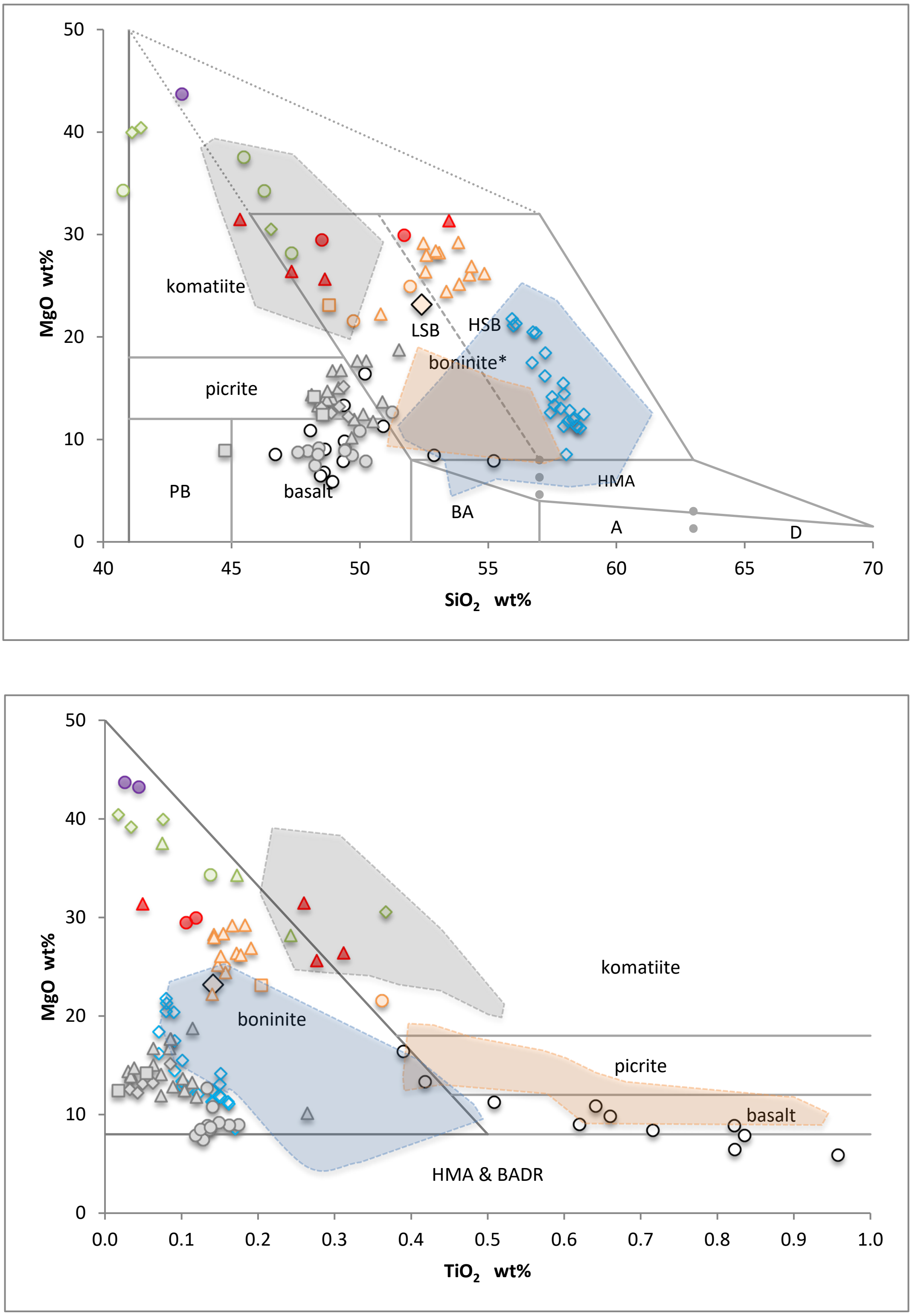

Fig. S8. Si-Mg-Ti plots, used in recent boninite classification (Pearce & Reagan, 2019). AN-1 consistently plot as a LSB. Calculations according to Pearce & Reagan (2019). All other samples of this study plotted for reference. Abbreviations: LSB – Low-silica boninite, HSB – High-silica boninite, PB – picrobasalt, BA – basaltic andesite, HMA – High-Mg andesite, A – andesite, D – Dacite, BADR – Basalt-andesite-dacite-rhyolite, SHMB – siliceous high-Mg basalt, LOTI – low-Ti basalt. Other symbols and references as in **Fig. 4.**

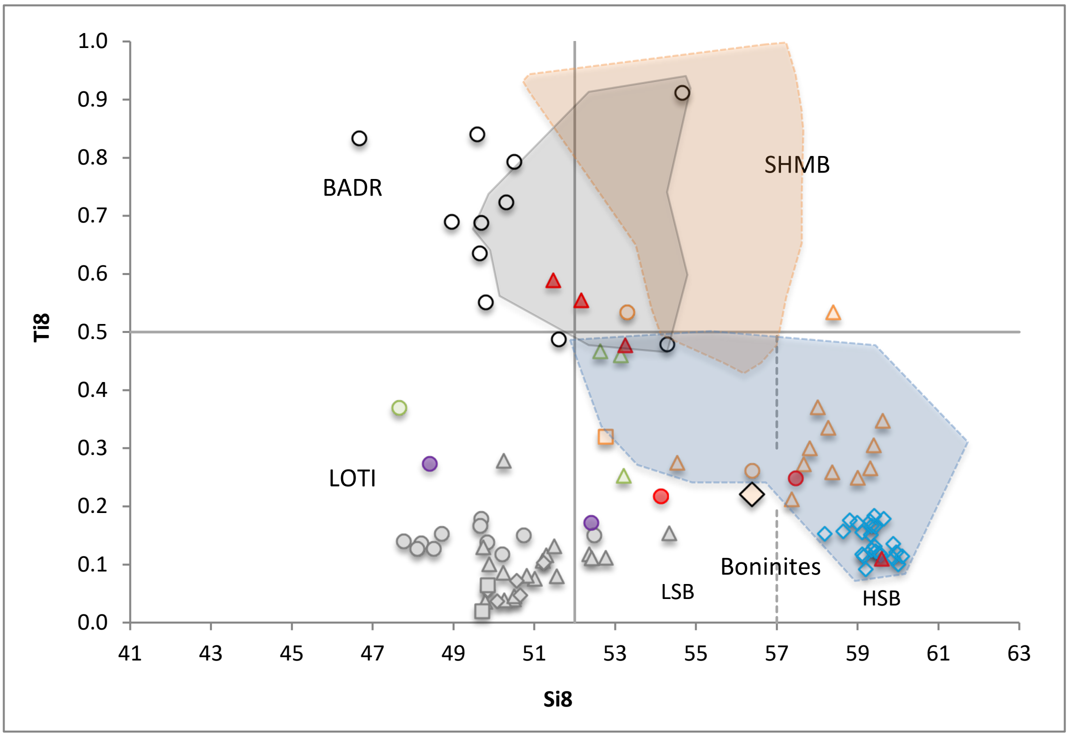

Fig. S8 (continued). Si_8-Ti_8 plots, used in recent boninite classification (Pearce & Reagan, 2019).

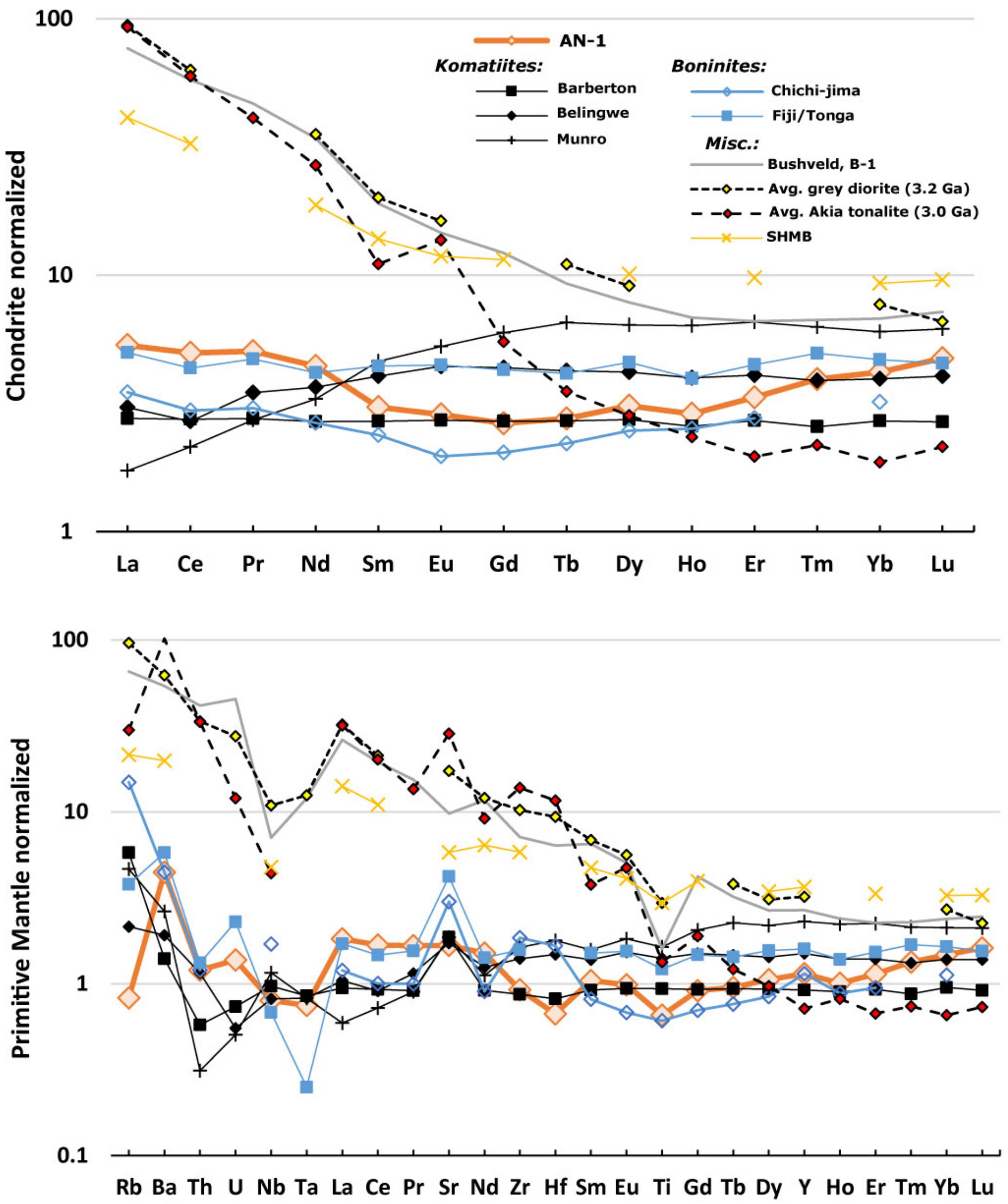

Fig. S9. Primitive mantle normalised cumulate models. The models are identical to those in **Fig. 13** of the main text – see this figure caption for details.

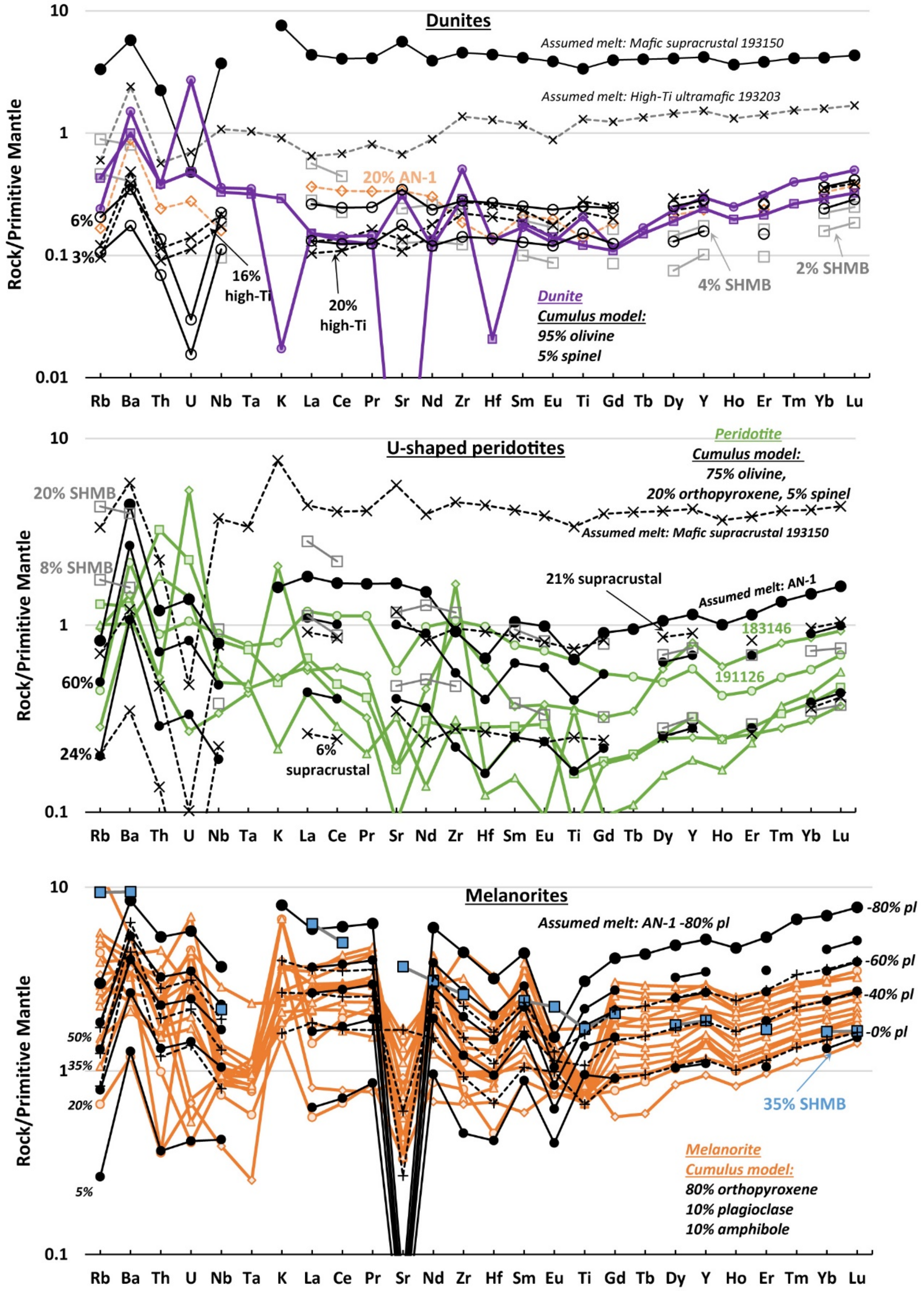

Fig. S10. Primitive mantle normalised cumulate models. The models are identical to those in **Fig. 13** of the main text – see this figure caption for details.

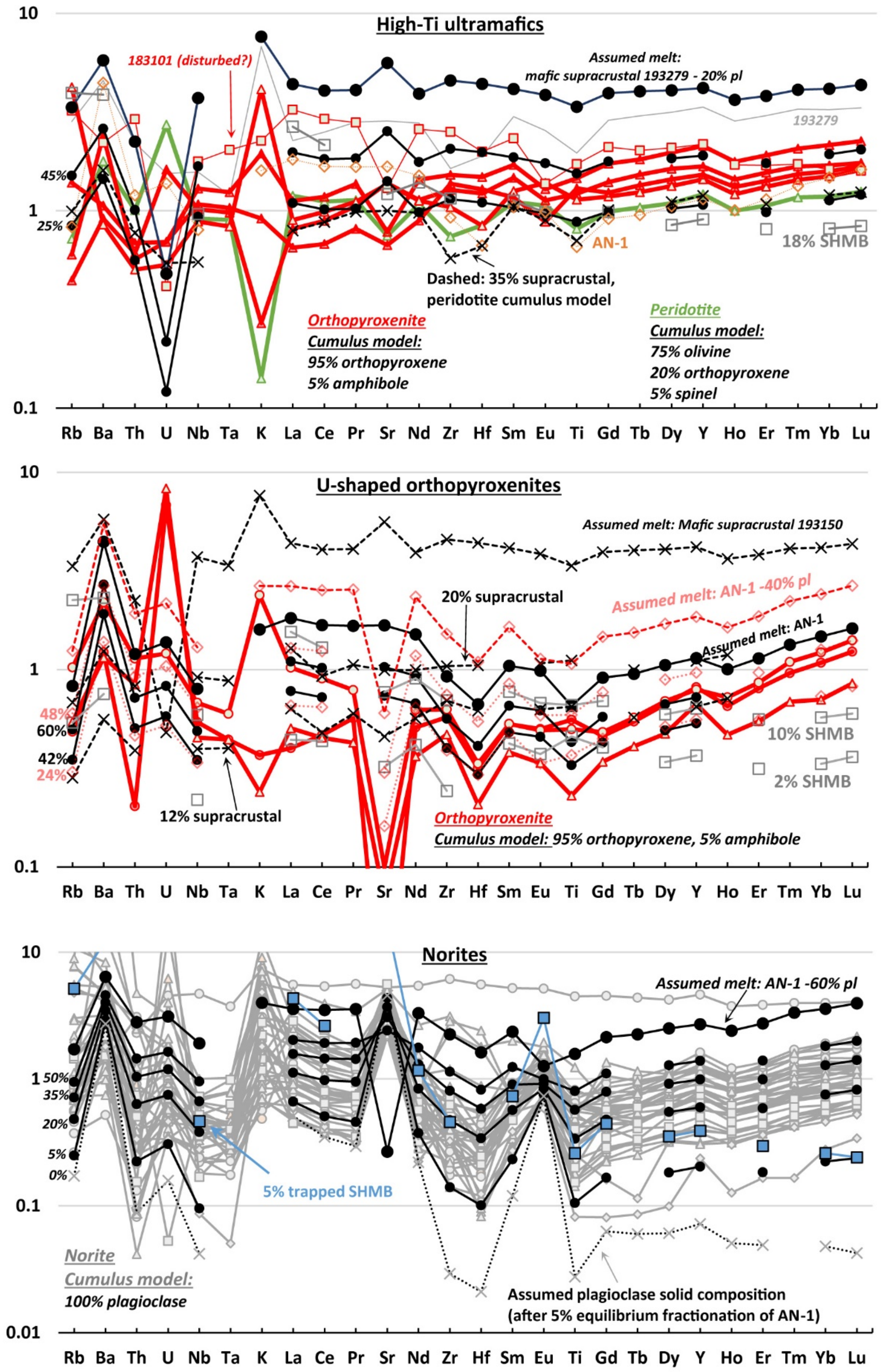

Fig. S10 (continued). Primitive mantle normalised cumulate models.

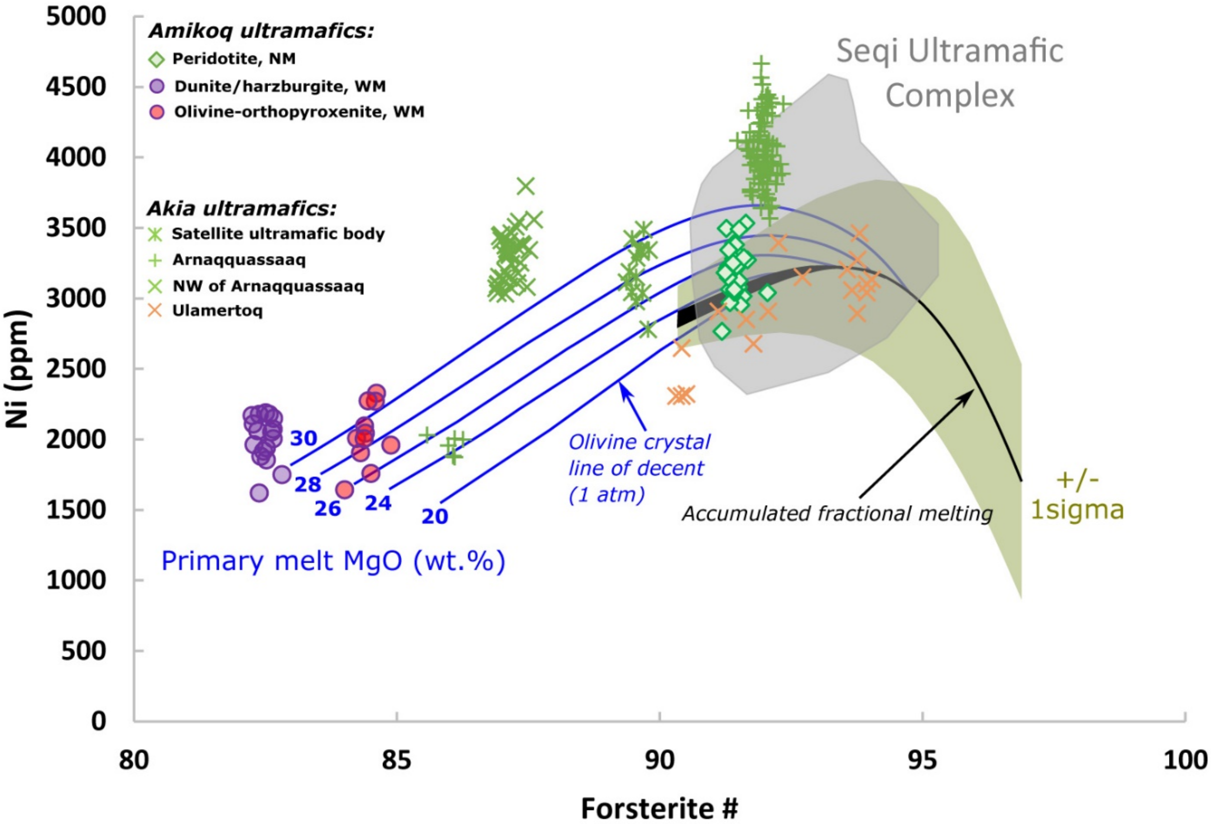

Fig. S11. Ni and forsterite content ($Mg^{2+}/(Mg^{2+}+Fe^{2+})$) in Fiskefjord olivine superimposed on **Fig. 5** of Herzberg et al. (2016). Black line is accumulated fractional melting (green area correspond to 1 sigma), blue lines are olivine crystal lines of decent at 1 atmosphere for melts with 20 to 30 wt.% MgO. Most of the Fiskefjord olivine data may in principle be explained as cumulates associated with high-MgO melts. Arnaqquassaaq is indicated in **Fig. 2**, and “Satellite bodies” refer to minor ultramafic occurrences in the vicinity of Amikoq. Data sources: Guotana et al. (2018); Szilas et al. (2018), others as in **Fig. 5**.

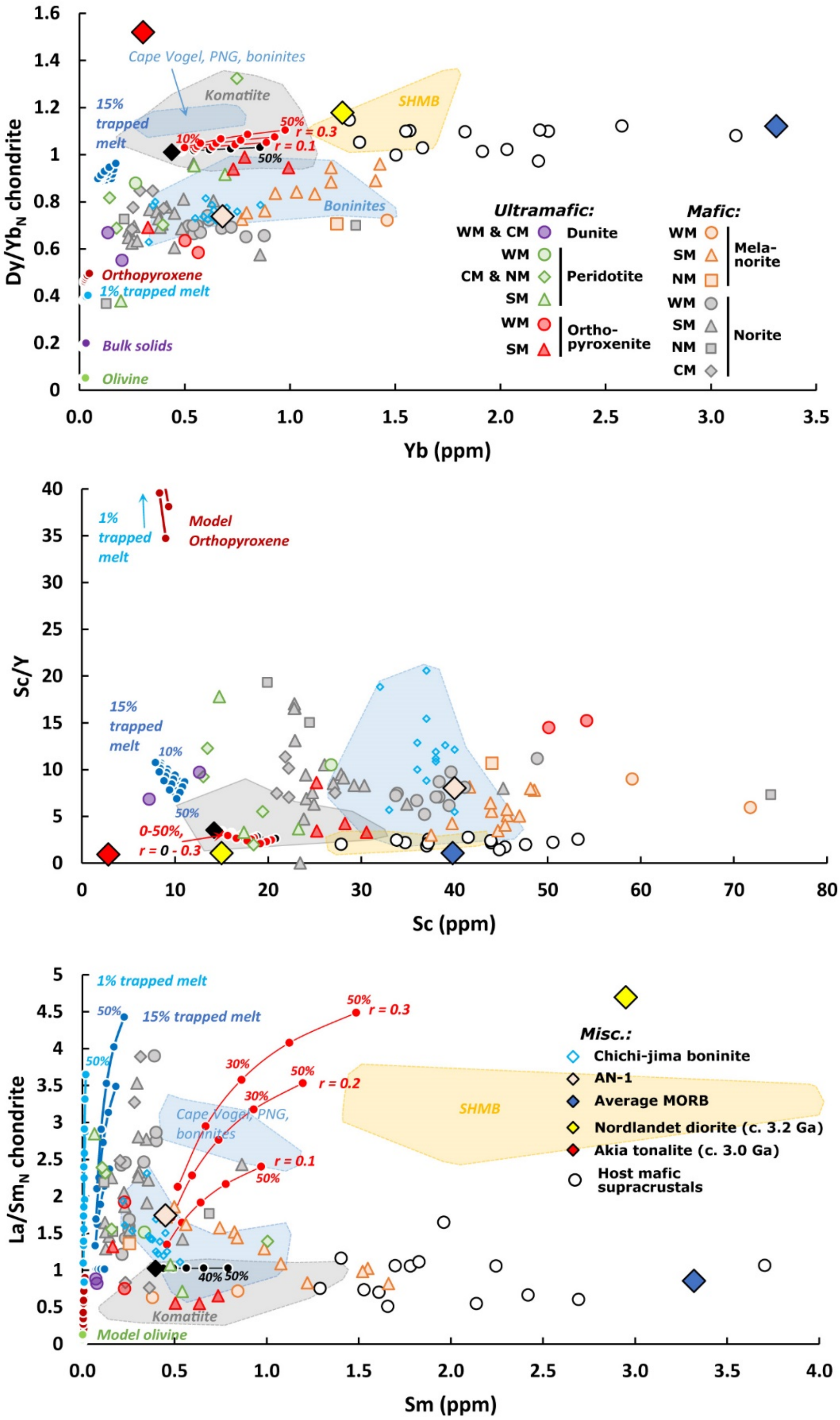

Fig. S12. Supplementary plots of AFC modelling involving an assumed komatiite parental melt and average Akia tonalite as contaminant. The modelled melts demonstrate that the boninitic AN-1 cannot be reproduced through contamination of a komatiite, especially well illustrated in terms of Dy/Yb and Sc/Y. See caption of **Fig. 12** and main text for details

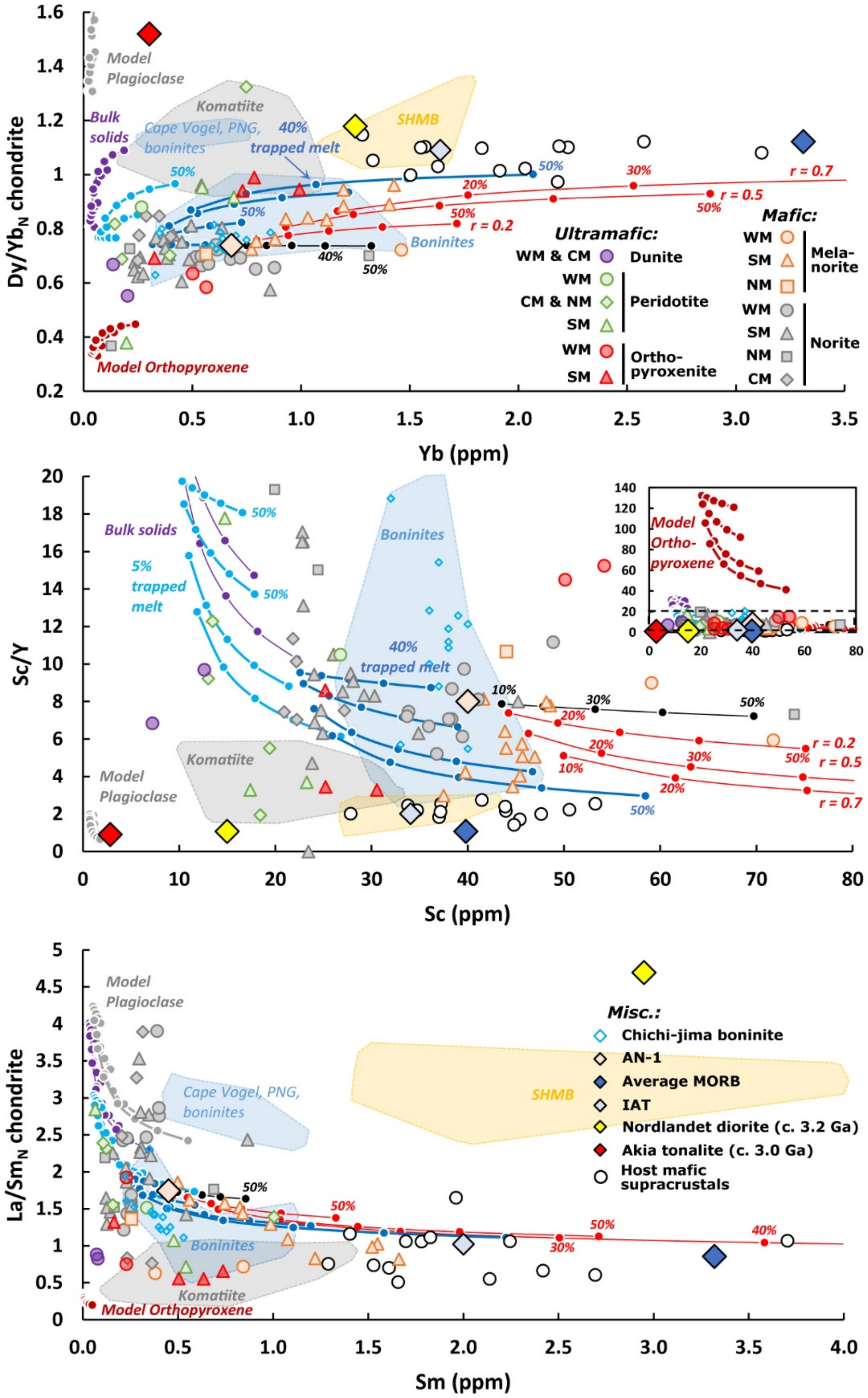

Fig. S13. Supplementary plots of AFC modelling and accumulation involving boninitic AN-1 parental melt and an IAT as contaminant. The melanorite data require a contaminant of MORB-like character but with elevated La/Nb, modelled here as an IAT. The norites are predominantly plagioclase cumulates though South Margin norites may require a relatively higher orthopyroxene content, evidenced from lower Dy/Yb and La/Sm. See caption of **Fig. 13** and main text for details.

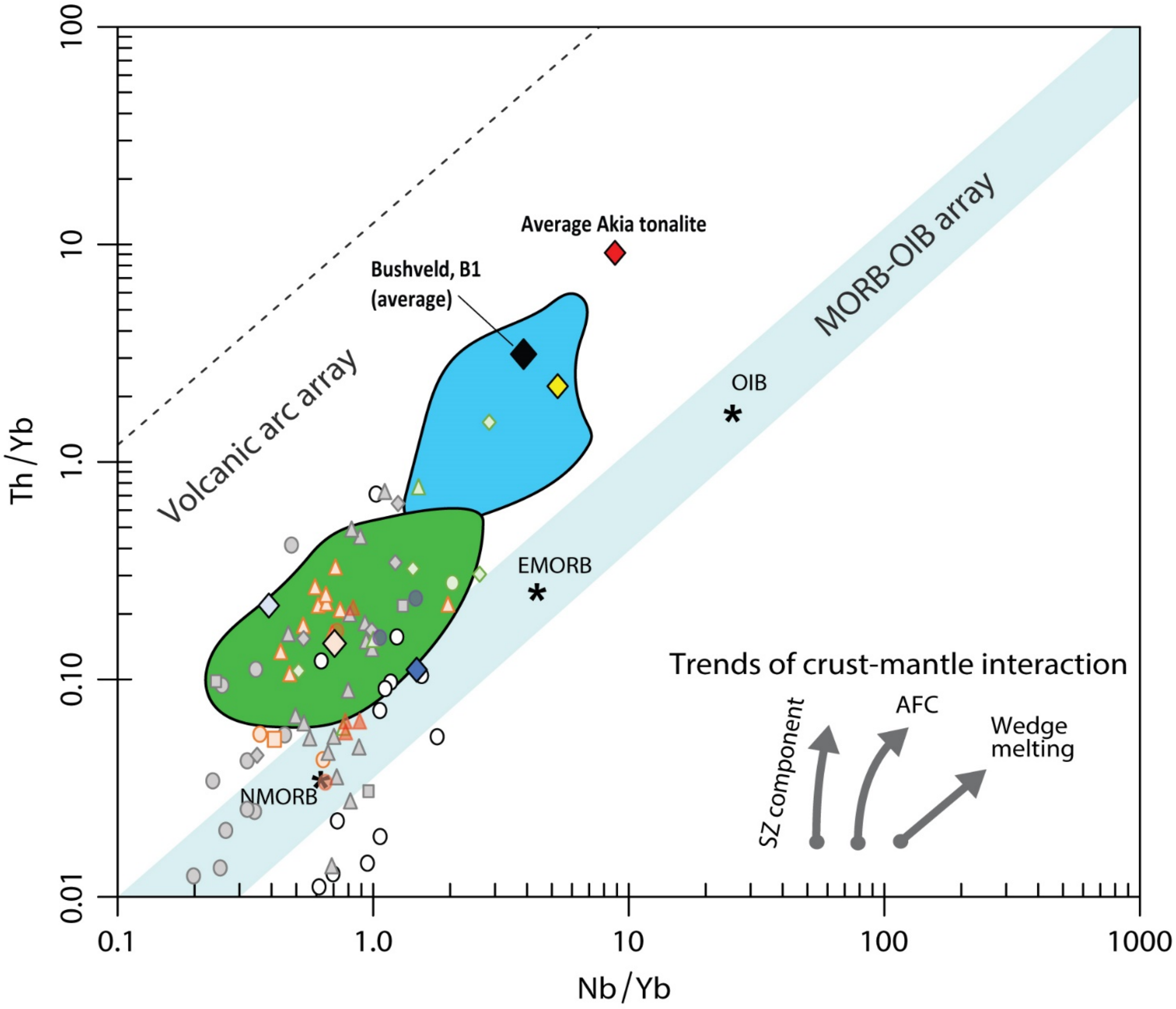

Fig. S14. Tectonic discrimination diagram (after Pearce, 2008). Symbols are the same as in previous diagrams, and the green and blue fields are the extent of tholeiitic metabasalts and calc-alkaline metaandesites of Szilas (2018), respectively.

References

Aarestrup, E., Jørgensen, T.R., Armitage, P.E., Nutman, A.P., Christiansen, O. and Szilas, K., 2020. The Mesoarchean Amikoq Layered Complex of SW Greenland: Part 1. Constraints on the P–T evolution from igneous, metasomatic and metamorphic amphiboles. Mineralogical Magazine, 84(5), pp.662-690.

Guotana, J.M., Morishita, T., Yamaguchi, R., Nishio, I., Tamura, A., Tani, K., Harigane, Y., Szilas, K. and Pearson, D.G., 2018. Contrasting textural and chemical signatures of chromitites in the Mesoarchaean Ulamertoq peridotite body, southern West Greenland. Geosciences, 8(9), p.328.

Herzberg, C., Vidito, C. and Starkey, N.A., 2016. Nickel–cobalt contents of olivine record origins of mantle peridotite and related rocks. American Mineralogist, 101(9), pp.1952-1966.

Kristensen, T. En geologisk og geokemisk tolkning af mafiske og ultramafiske bjergarter og deres økonomiske mineralpotentiale, Fiskefjordsregionen, sydlige Vestgrønland (Unpublished M.Sc. thesis), Aarhus University; 2006. 135 pp.

Pearce, J.A. 2008. Geochemical fingerprinting of oceanic basalts with applications to ophiolite classification and the search for Archean oceanic crust. Lithos, 100(1-4), 14-48.

Pearce, J.A. and Reagan, M.K., 2019. Identification, classification, and interpretation of boninites from Anthropocene to Eoarchean using Si-Mg-Ti systematics. Geosphere, 15(4), pp.1008-1037.

Szilas, K., Kelemen, P.B. and Bernstein, S., 2015. Peridotite enclaves hosted by Mesoarchaean TTG-suite orthogneisses in the Fiskefjord region of southern West Greenland. GeoResJ, 7, pp.22-34.

Szilas, K., 2018. A geochemical overview of mid-Archaean metavolcanic rocks from southwest Greenland. Geosciences, 8(7), p.266.

Szilas, K., van Hinsberg, V., McDonald, I., Næraa, T., Rollinson, H., Adetunji, J. and Bird, D., 2018. Highly refractory Archaean peridotite cumulates: Petrology and geochemistry of the Seqi Ultramafic Complex, SW Greenland. Geoscience Frontiers, 9(3), pp.689-714.